Received: 26 October 2021 | Revised: 11 January 2022 | Accepted: 12 January 2022

DOI: 10.1002/biot.202100577

Biotechnology Journal

RESEARCH ARTICLE

Direct capture and selective elution of a secreted polyglutamate-tagged nanobody using bare magnetic nanoparticles

Alexander A. Zanker[1] | **Patrick Stargardt**[2] | **Sophie C. Kurzbach**[1] | **Chiara Turrina**[1] | **Juergen Mairhofer**[2] | **Sebastian P. Schwaminger**[1] | **Sonja Berensmeier**[1]

[1] Bioseparation Engineering Group, Department of Mechanical Engineering, Technical University of Munich, Garching, Germany

[2] enGenes Biotech GmbH, Vienna, Austria

Correspondence
Sonja Berensmeier, Bioseparation Engineering Group, Department of Mechanical Engineering, Technical University of Munich, Boltzmannstr. 15, 85748 Garching, BY, Germany.
Email: s.berensmeier@tum.de

Funding information
Federal Ministry of Education and Research, Grant/Award Number: 031B0521A; Marie Skłodowska Curie actions of the European Commission, Grant/Award Number: 887412

Abstract

Background: The secretion and direct capture of proteins from the extracellular medium is a promising approach for purification, thus enabling integrated bioprocesses.

Major Results: We demonstrate the secretion of a nanobody (VHH) to the extracellular medium (EM) and its direct capture by bare, non-functionalized magnetic nanoparticles (MNPs). An ompA signal peptide for periplasmic localization, a polyglutamate-tag (E_8) for selective MNP binding, and a factor Xa protease cleavage site were fused N-terminally to the nanobody. The extracellular production of the E_8-VHH (36 mg L^{-1}) was enabled using a growth-decoupled *Escherichia coli*-based expression system. The direct binding of E_8-VHH to the bare magnetic nanoparticles was possible and could be drastically improved up to a yield of 88% by adding polyethylene glycol (PEG). The selectivity of the polyglutamate-tag enabled a selective elution of the E_8-VHH from the bare MNPs while raising the concentration factor (5x) and purification factor (4x) significantly.

Conclusion: Our studies clearly show that the unique combination of a growth-decoupled *E. coli* secretion system, the polyglutamate affinity tag, non-functionalized magnetic nanoparticles, and affinity magnetic precipitation is an innovative and novel way to capture and concentrate nanobodies.

KEYWORDS
affinity peptide tag, downstream processing, magnetic iron oxide nanoparticles, PEG, secretion

1 | INTRODUCTION

Nanobodies, often termed single domain antibodies (sdAb) or variable domain of heavy-chain antibodies (VHH), have attracted great interest in recent years by showing remarkable advantages over usual antibodies.[1,2] The most obvious advantage is their small size enabling an easier penetration of tissues. Additionally, they have access to

Abbreviations: ATPS, aqueous two-phase system; BCA, bicinchoninic acid; DLS, dynamic light scattering; EM, extracellular medium; E_8, polyglutamate tag with eight glutamates; IB, inclusion bodies; Fwd, forward primer; MNPs, magnetic iron oxide nanoparticles; ompA, outer membrane protein A; P, pellet; PBCA, modified BCA assay for particles; PCR, polymerase chain reaction; PEG, polyethylene glycol; Rev, reverse primer; SP, spheroplast; VHH, variable domain of a heavy chain antibody

antigens which are hardly accessible for bigger antibodies, for example, active sites of enzymes.[3] Other beneficial properties have also propelled this research (e.g., the inherent thermal and chemical stability, the expression in microorganisms, and their low immunogenicity).[4–7] On top of that, nanobodies can be expressed in many different organisms, including *Escherichia coli*.[8] In contrast, conventional antibodies are mostly expressed in mammalian cell lines due to their need for post-translational modifications (e.g., glycosylation).[9] The expression in microorganisms, especially *E. coli*, is often faster and more cost-efficient than other expression systems, like the expression in mammalian cell lines.[10] However, one problem is the inclusion body (IB) formation of nanobodies when expressed in the cytoplasm and which needs further processing to result in functional nanobodies.[8,11] The IB formation can be bypassed through periplasmic expression, which is the most popular route for nanobodies.[8]

For further purification, nanobodies secreted into the periplasm need to be released.[10] To save an additional periplasmic release step, various approaches exist to secrete proteins to the extracellular medium for *E. coli* (e.g., a higher membrane permeability, co-expression of lysis proteins, hemolysin secretion).[12,13] Recently, the enGenes-X-press strain (*E. coli* BL21(DE3) derivative) has proven to be highly promising for extracellular expression of proteins, especially nanobodies.[14,15] The secretion mechanism of the enGenes expression system is ascribed to the outer membrane leakiness. This leakiness is achieved by inhibiting the *E. coli* RNA polymerase and resulting in growth-decoupled production of recombinant proteins.[14] After the secretion, nanobodies are usually purified by immobilized metal affinity chromatography or ion exchange chromatography.[11,12,16] However, chromatographic methods are often costly.[17,18] In contrast, the use of magnetic nanoparticles (MNPs) is suggested to be a cost-efficient and promising alternative as it combines magnetic properties with a high specific surface area, a fast and simple handling, and easy upscale possibilities.[17,19–21] MNPs are applied in many nano-bio applications with a functionalized surface, however, functionalization is costly.[21,22] Therefore, the use of bare, non-functionalized MNPs saves costs and appears to be worthwhile.[23] Especially for sustainability reasons, it makes sense to use non-functionalized MNPs, since no toxic ligands are needed. In previous studies, a peptide tag consisting of repeating glutamates (E_6) showed a high affinity towards bare MNPs and an adsorption behavior appropriate for purification.[24,25] The strong binding can be ascribed to the bridging coordination and electrostatic attractions of the glutamates and MNPs.[25,26] As in immobilized metal affinity chromatography (IMAC), a peptide tag is added, however, stationary phase functionalization is omitted, and a hazardous substance, like imidazole, is not needed for elution.

In a proof of principle, an E_6-tagged GFP (E_6-GFP) was purified with bare MNPs in a high gradient magnetic separation (HGMS).[27] Recently, researchers observed improved capturing efficiency with magnetic particles by combining it with precipitation, naming that approach 'affinity magnetic precipitation'.[28] Santos et al. could enhance the yield and purity of captured antibodies by adding polyethylene glycol (PEG).[28] The approach by Santos et al. is based on functionalized magnetic particles, whereas the magnetic nanoparticles in this study are non-functionalized.[28] The combination of PEG and magnetic particles is also known in magnetic aqueous two-phase systems (ATPS), where magnetic particles are known to enhance the phase separation[29,30] or bind proteins when being functionalized.[31–33] Aside those two downstream applications, PEG is commonly known to precipitate proteins by steric exclusion and even allows for an improved retention of proteins to the chromatographic material.[34–36]

In this manuscript, we molecularly fused the signal peptide ompA, the polyglutamate-tag (E_8) and a factor Xa cleavage site to the N-terminus of a nanobody. This allowed the nanobody to be secreted, to adsorb to bare magnetic nanoparticles and to enable the cleavage of the polyglutamate-tag. We have joined several highly promising approaches into one, resulting in a low-cost capturing approach for nanobodies with improved yields and distinctly enhanced purification and concentration factors. We achieved that by secreting the polyglutamate-tagged nanobody (E_8-VHH) with the enGenes-X-press system, capturing it by non-functionalized magnetic nanoparticles in the presence of PEG and selectively eluting the E_8-VHH. The unique symbiosis of the X-press strains, the magnetic nanoparticles and the polyglutamate-tag system promises a low-cost, rapid and transferable approach, not limited to nanobodies.

2 | MATERIALS AND METHODS

2.1 | Materials

All materials were used as supplied. *E. coli* BL21(DE3) (*E. coli* str. B F$^-$ ompT gal dcm lon hsdSB(rB$^-$mB$^-$) λ(DE3 [lacI lacUV5-T7p07 ind1 sam7 nin5]) [malB$^+$]K-12(λS)), enGenes-X-press-V1 (*E. coli* B F$^-$ ompT gal dcm lon hsdSB(rB$^-$ mB$^-$) λ(DE3 [lacI lacUV5-T7 gene 1 ind1 sam7 nin5]) attTN7:: < Para-Gp2 > ΔaraABCD),[15] and enGenes-X-press V2 (*E. coli* B F$^-$ ompT gal dcm lon hsdSB(rB$^-$mB$^-$) [malB$^+$]K-12(λS) araB::T7RNAP-tetA attTN7:: < Para-Gp2 >)[37] were used as expression organisms (enGenes Biotech GmbH, Austria). Magnetic nanoparticles were synthesized by co-precipitation of iron salts as described in previous work.[38] The provided silica-coated magnetic nanoparticles were synthesized and characterized, which is further described in the supplementary information (see SI). Oleate-coated magnetic nanoparticles were generated by assembling oleate and magnetic nanoparticles as described in Schwaminger et al.[39]

2.2 | Cloning

The VHH gene was integrated in a pET30 plasmid from enGenes.[15] The polyglutamate-tag (E_8) and the factor Xa protease cleavage site were fused between the ompA signal peptide and the N-terminal start codon of VHH via the Gibson assembly approach. A polymerase chain reaction (PCR) was performed to linearize the vector at the desired location (Fwd: GAAGTACAACTGCTGGAGA, Rev: GGCCTGCGCTACGGTA) using the Q5 High-Fidelity DNA Polymerase (New England Biolabs, USA). The NEBuilder HiFi DNA Assembly Kit was

used to assemble the linearized fragment with an oligo assembled fragment containing the polyglutamate-tag and the Xa protease cleavage site, as well as complementary ends to ompA-end and VHH-start nucleotides (TACCGTAGCGCAGGCCGAGGAAGAGGAAGAGGAAGAGGAAATTGAAGGCCGTGAAGTACAACTGCTGGAGA).

The resulting plasmid was transformed in *E. coli* DH5α cells with the TSS transformation protocol[40] and subsequently verified via sequencing (Eurofins Genomics GmbH, Germany). For further expression studies, the cloned pET30a_E_8-Xa-VHH plasmid was transformed (TSS transformation protocol) into different *E. coli*-derived strains (BL21(DE3), enGenes-X-press V1, enGenes-X-press V2).

2.3 | Growth experiment

The different strains' growth behavior (BL21(DE3), X-press V1, and X-press V2, all transformed with pET30a_E_8-VHH plasmid) was investigated in a BioLector (m2p Labs GmbH, Germany) micro fermentation system. The experimental procedure was carried out analogously to the studies by Stargardt et al.[15]

2.4 | Expression

Assessing the VHH expression in different strains, the transformed BL21(DE3) and X-press V1 were cultivated at 30°C for several hours in shaking flasks (40 mL) containing semisynthetic (SS) medium with 30 mg L^{-1} kanamycin. The composition of the SS medium is described elsewhere.[41] Expression was induced by the addition of 0.5 mM IPTG and 100 mM Arabinose (only X-press V1) after reaching an OD_{600} between 0.6 and 0.9. X-press V2 strains were cultivated in autoinduction medium (20 g L^{-1} Tryptone, 5 g L^{-1} Yeast extract, 5 g L^{-1} NaCl, 6 g L^{-1} Na_2HPO_4, 3 g L^{-1} KH_2PO_4, 10 mL 60% Glycerol, 5 mL 10% Glucose) with varying arabinose concentrations (1.5%, 1% (w/v)) for 3 days at 30°C and at different scales (40 and 300 mL). The cultivation broth was centrifuged (3000 × *g*, 30 min), resulting in a pellet and a supernatant (designated as the extracellular medium, EM). The pellet was further treated with chloroform for periplasmic release and centrifuged (17,000 × *g*, 30 min) to separate the periplasmic fraction (supernatant) from the spheroplast (pellet).[42] The chloroform treatment includes the resuspension of the pellet in 99% chloroform (volume: 1% of total cultivation volume), incubation for 15 min at RT, and the addition of Tris buffer (50 mM, pH 8.0, 10% of cultivation volume). The different fractions were analyzed with sodium dodecyl sulfate-polyacrylamide gel electrophoresis (SDS-PAGE). The protein concentration of the EM was obtained by the Bradford assay.[43]

2.5 | Batch adsorption experiments

The binding of the proteins from the EM to the MNPs was assessed by mixing different concentrations of EM to a final concentration of 1 g L^{-1} MNPs. The MNPs stored in Tris (50 mM, pH 7.0) or acetate buffer (50 mM, pH 7.0, 6.0, 5.5) were poured into a 2 mL Eppendorf tube. The storage buffer was removed by applying a magnetic field and the EM was added, resulting in a final volume of 1.8 or 0.5 mL. The pH of the EM was adjusted with HCl beforehand. PEG 6000 (10% (w/v)) was added to the EM before pH adjustment, in the case of PEG-containing samples. The EM-MNP mixture was incubated for 1 h (25°C, 1000 rpm), a magnetic field was applied, and the supernatant was removed. The remaining MNPs were washed twice and resuspended in Tris buffer (50 mM, pH 7.0, initial volume). Samples were taken for BCA analysis and SDS-PAGE.

The total amount of the proteins bound to the MNPs was determined with a particle BCA (PBCA, described in Section 2.6), and was related to the MNP amount (total protein load, $g_{Protein}\ g_{MNP}^{-1}$). The bound VHH was calculated from the load multiplied with the purity of VHH. The purity of VHH was obtained by densitometric analysis via SDS-PAGE. If not stated otherwise, every sample was performed as technical duplicates, and measured as analytical triplicates for the PBCA and SDS-PAGE as one analytical replicate. Elution of MNP-bound proteins was performed by resuspending the MNPs in phosphate-buffered saline (100 mM phosphate, 137 mM NaCl, 2.7 mM KCl, pH 8.5, 5% of initial volume), incubating the mixture over night and magnetically separating the supernatant (eluate) from the MNPs.

Reference experiments were performed without magnetic nanoparticles and with silica- and oleate-coated magnetic nanoparticles, respectively. Furthermore, the reference experiments were carried out at 10% PEG 6000 and pH 5.5. The oleate-coated magnetic nanoparticles were separated by centrifugation (5000 × g, 5 min).

2.6 | Protein analytics (SDS-PAGE, BCA, Bradford, mass spectrometry)

A modified bicinchoninic acid (BCA) assay was carried out to determine the concentration of protein bound to the MNPs. The BCA on particles (designated as particle BCA (PBCA)) required the separation of the MNPs from the BCA assay after reaction using a 96-well filter plate (0.2 μm). The reagents from the Pierce BCA protein assay kit (Thermo Fisher Scientific Inc., USA) were used. The obtained values were blanked with references (MNPs incubated with autoinduction medium, PEG, and washed with Tris buffer). The protein concentration of the EM was obtained via Bradford assay. For this, 10 μL samples were loaded onto a 96-well microtiter plate as analytical quintuplicates, 300 μL of the Bradford reagent was added, and the optical density at 595 nm was measured via an Infinite M200 Microplate Reader (Tecan Deutschland, Germany). The purity of E_8-VHH was determined by densitometric analysis of SDS-PAGE. The samples were prepared by mixing the sample with 2x SDS loading buffer (containing 10 mM DTT) and boiled for 5 min at 95°C. 10 μL of the prepared samples were loaded onto a 15% polyacrylamide gel. After the run (150 V, 100 min), the gel was scanned with an Amersham Typhoon NIR Plus (GE Healthcare Europe GmbH, Germany) and densitometrically analyzed with the Image Quant TL software. Samples of the SP or pellet were loaded with a final concentration of OD 8, MNP bound samples

with 10 g L^{-1}, periplasmic fraction, and EM were concentrated with 5000 Da Vivaspin columns (Sartorius AG, Germany). Samples for mass spectrometry were prepared according to the protocol described by Shevchenko et al.[44] The prepared samples were analyzed with LC-MS as published by Wiśniewski and Mann.[45] The yield was calculated from the E_8-VHH amount bound to the magnetic nanoparticles and divided by the E_8-VHH amount present in the EM. The purification factor was the ratio of the MNP-bound E_8-VHH purity to the E_8-VHH purity in the EM. The concentration factor specified the ratio of E_8-VHH concentration in the EM divided through the E_8-VHH concentration in the eluted sample.

2.7 | Particle characterization (Zeta, DLS, FT-IR)

The agglomeration behavior and zeta potential of the magnetic nanoparticles in different environments was determined via a Zeta-Sizer Ultra (Malvern Pananalytical, United Kingdom). The dynamic light scattering of 1 mL MNPs (1 g L^{-1}) was measured in a standard cuvette as technical duplicates and analytical triplicates each. The accessible specific surface area (S_m) of particle agglomerates was estimated assuming the agglomerate as a sphere and 5.18 g cm^{-3} as the density ($S_m = \frac{6}{d*\rho}$). The zeta potential of MNPs was measured in technical duplicate and analytical quintuplicate each in a DTS1080 cuvette (disposable folded capillary cell). To calculate the zeta potential, a refractive index of 1.330, a dynamic viscosity of 0.887 mPa s, and a dielectric constant of 78.5 F m^{-1} were used. For PEG-containing samples, the dynamic viscosity was altered (2.545 mPa s).[46] Infrared spectra (4000–400 cm^{-1}) of MNP samples (two times washed and resuspended in Tris buffer (50 mM, pH 7.0) in a final concentration of 5 g L^{-1}) were recorded with a Bruker FT-IR Alpha II with a single reflection Platinum-attenuated total reflection (ATR) accessory (Bruker Optics GmbH, Germany). The baselines were corrected (concave rubber band method) using the software OPUS 8.1.

3 | RESULTS AND DISCUSSION

3.1 | Extracellular expression of E_8-VHH by X-press strains

The first goal was to secrete the polyglutamate-tagged nanobody (ompA-E_8-VHH, see Figure 1A) to the EM. This secretion is achieved by secreting the E_8-VHH to the periplasm (SEC-pathway), which then leaks into the EM through the leaky outer cell membrane of the enGenes-X-press system (see Figure 1B).[14]

The growth of the enGenes-X-press strains and the secretion of the E_8-VHH were compared with the well-known *E. coli* BL21(DE3), which served as a benchmark. Without arabinose and IPTG, all strains showed a similar growth behavior, with all having a final biomass of approx. 10–12 g L^{-1} in BioLector micro fermentation experiments (see Figure 1C). As intended, the presence of arabinose had an inhibitory effect on the X-press strains showing higher cell dry masses at lower arabinose concentrations and the highest cell dry mass being in the absence of arabinose and IPTG (see Figure S1). These findings are in good agreement with the literature explaining the arabinose influence on X-press strains leading to a growth-decoupled expression of the protein of interest.[15,37] The VHH producing strain and the untransformed control strain showed no growth limitations in shaking flask experiments (see Figure S2). E_8-VHH was strongly expressed as inclusion bodies in all three different strains (Figure 1D), which is indicated by the intense spot at around 18 kDa in the SP samples and is a common phenomenon for nanobodies.[8,48,49] While the BL21(DE3) strain could not secrete the E_8-VHH to the EM, both X-press strains succeeded showing a weak spot in the height of around 15.7 kDa (see Figure 1D, lanes 6 and 9). Periplasmic expression of the E_8-VHH, though, was also possible with BL21(DE3) (see Figure S3). For unambiguous identification of the E_8-VHH, the colored curls in Figure 1D were analyzed via mass spectrometry. The E_8-VHH could be identified in the 18 kDa (red, SP) and in the 15.7 kDa spot (blue, EM) with the highest scores (see Figure S4). Additionally, the E_8-tag was found in both spots. The 37 kDa spot (orange, EM) was identified as porine gram-negative type. In addition to secretion, the straightforward expression of the E_8-VHH in autoinduction medium using X-press V2 was advantageous as it required minimal effort and enabled a strong expression representing up to 62% of total protein in the SP and 36 mg_{VHH} $L_{cultivation}{}^{-1}$ (in shaking flasks) in the EM (see Figure S5). The expression yield is comparable or higher than references which also expressed VHH in *E. coli*.[5,11,50,51] Furthermore, expressions using the BioLector micro fermentation system yielded 75 mg_{VHH} $L_{cultivation}{}^{-1}$ with X-Press strains which was about twice as high as the corresponding BL21(DE3) yield (see Table S1). Our findings strongly suggest the usage of X-press strains for extracellular expression. The secretory potential of the X-press strains has already been shown for other proteins and promises a superior behavior over the commonly used BL21(DE3).[14]

3.2 | Capturing of E_8-VHH by affinity magnetic separation

A protein with relatively low concentration faces tremendous competition in an EM when binding to magnetic nanoparticles. Despite the relatively low abundance of E_8-VHH (8% purity), we were able to capture the E_8-VHH with bare MNPs directly from the EM. However, the yield was low (20%), and a pH adjustment did not enhance the yield (see Figure 2).

At least, the pH adjustment did increase the yield to 20% from initially 8% in a not pH-adjusted EM (pH 7.8). We could enhance the yield significantly by adding 10% (w/v) PEG 6000 and applying an acidic pH resulting in 88% of captured E_8-VHH (see Figure 2). Improved yields upon PEG addition were also reported by Santos et al. who combined protein precipitation through PEG with affinity interactions of antibodies and triazine-functionalized magnetic particles.[28] We chose 10% PEG 6000 since smaller proteins tend to precipitate with larger PEG sizes and higher concentrations, and we found 10% PEG 6000 to be sufficient.[35,36] We investigated the influence of the PEG on the

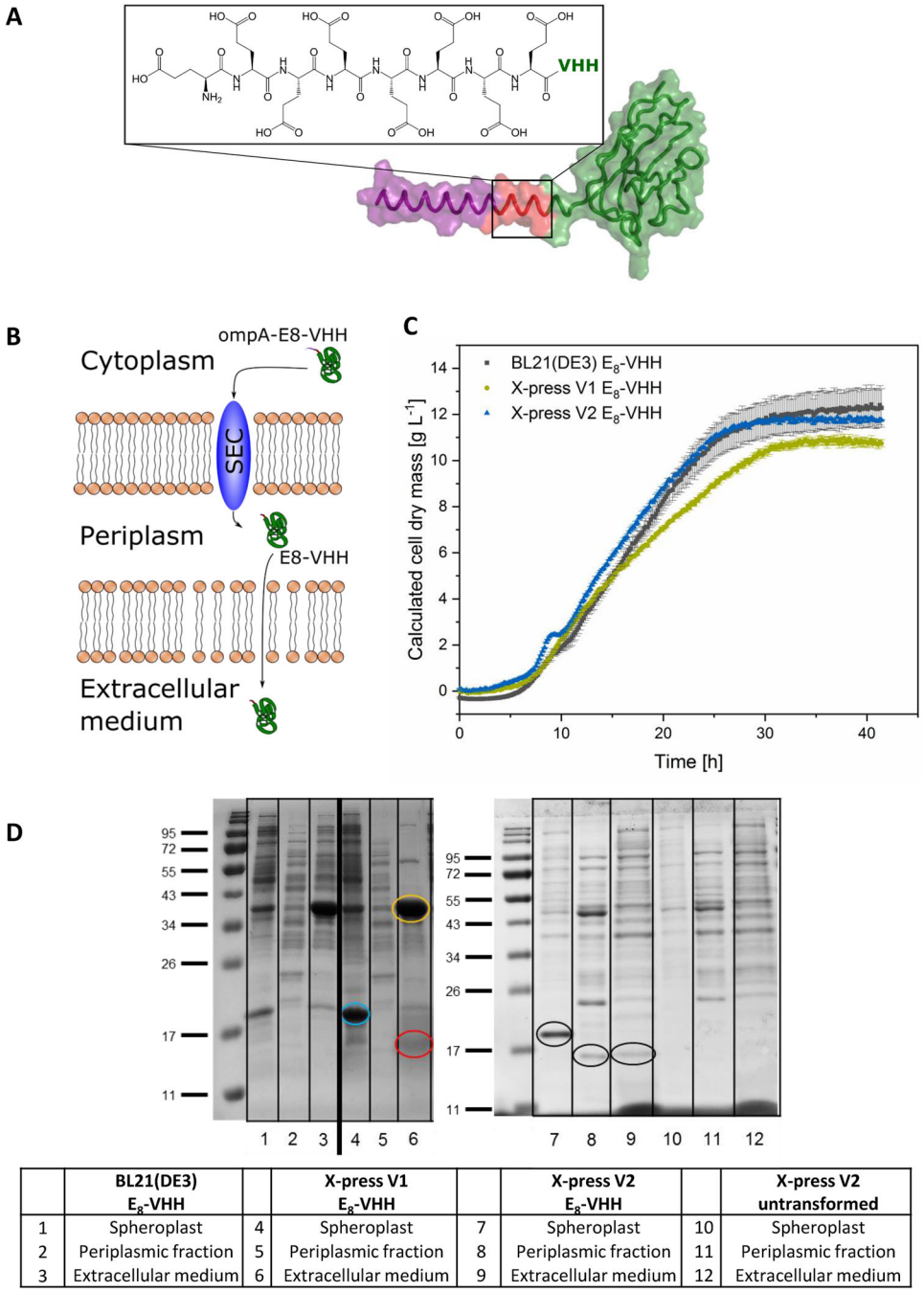

	BL21(DE3) E_8-VHH		X-press V1 E_8-VHH		X-press V2 E_8-VHH		X-press V2 untransformed
1	Spheroplast	4	Spheroplast	7	Spheroplast	10	Spheroplast
2	Periplasmic fraction	5	Periplasmic fraction	8	Periplasmic fraction	11	Periplasmic fraction
3	Extracellular medium	6	Extracellular medium	9	Extracellular medium	12	Extracellular medium

FIGURE 1 Scheme of the E_8-VHH, the secretion and data to the growth of X-press strains and extracellular expression of E_8-VHH. (A) The chemical structure of the E_8-tag (Glu-Glu-Glu-Glu-Glu-Glu-Glu-Glu) and the tertiary structure of the ompA-E_8-VHH using Robetta for simulation and PyMol for visualization.[47] Purple = ompA, red = E_8-tag, green = VHH. (B) Scheme of secretion of E_8-VHH via the SEC-pathway to the periplasm and the subsequent leaking into the extracellular medium. (C) Comparison of the growth behavior of BL21(DE3) and both X-press strains (V1 and V2) bearing the E_8-VHH plasmid. Strains were grown in biological duplicates in a BioLector micro fermentation system with 48-well flower plates. Cultivation in a feed-in-time (FIT) fed-batch medium without arabinose and IPTG addition. Samples were measured every 10 min, and the cell dry mass (CDM) was calculated by linearly regressing scattered light signals. (D) SDS-PAGEs of E_8-VHH cultivated in *E. coli* BL21(DE3), X-press V1, X-press V2, and untransformed X-press V2. BL21(DE3) and X-press V1 were cultivated in semisynthetic medium, X-press V2 samples in autoinduction medium. Different fractions (spheroplast and periplasmic fraction after chloroform treatment, extracellular medium) were loaded on a 15% polyacrylamide gel. The thick black line between the lanes 3 and 4 (left gel) indicates that three additional lanes were cropped. The original gel is displayed in the SI. The colored curls were analyzed with mass spectrometry (fingerprinting) additionally. The black curls show the E_8-VHH expressed in X-press V2. No such spots in the reference (lanes 10–12)

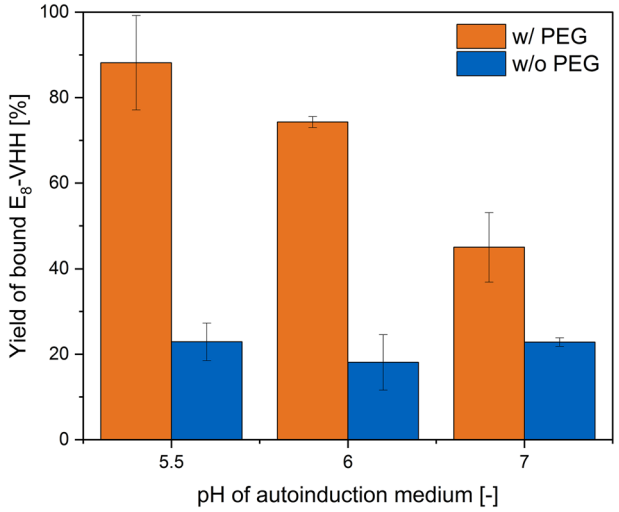

FIGURE 2 Yield of E_8-VHH bound to MNPs dependent on pH and PEG. E_8-VHH was expressed in X-press V2, the extracellular medium separated from the cells, the pH adjusted, and a final protein concentration of 0.25 g L^{-1} was incubated with 1 g L^{-1} MNPs (1 h, 1000 rpm, 25°C). PEG samples contained 10% (w/v) PEG 6000, added before pH adjustment. The yield was obtained by the ratio $m_{VHH,\,bound}/m_{total\ VHH\ in\ EM}$. The total protein load was obtained from technical duplicates measured in analytical triplicate via particle-BCA each. The amount of E_8-VHH is the product of the total protein amount and the purity of E_8-VHH. The latter derives from technical duplicates analyzed densitometrically with SDS-PAGE

magnetic nanoparticles and on the proteins to further evaluate the observed phenomenon. The alteration of pH and the addition of PEG influenced the total protein binding, and in return, the yield of captured E_8-VHH. Clearly, the presence of PEG led to higher total protein (125 mg g^{-1}) and E_8-VHH load (17 mg g^{-1}), which resulted in the observed higher yields (see Figure 3A). The results further show a higher total protein load at the more acidic pH (pH 5.5) than at pH 7.0 for PEG- and no PEG-containing samples (see Figure 3A). Schwaminger et al. and Blank-Shim et al. have also observed an increasing load at decreasing pH for the polyglutamate peptide tag and a polyglutamate-tagged GFP.[25,27]

The question arises if the higher protein loads and yields were a consequence of the changed magnetic nanoparticle and / or protein behavior. The behavior of the magnetic nanoparticles was analyzed with a ZetaSizer. When resuspended in Tris or autoinduction medium, the MNPs agglomerate and form sizes of around 2700 to 3400 nm, contrasting to a size of approx. 96 nm in water (Table S2). The presence of PEG led to smaller MNP agglomerates (see Figure 3B). However, no significant change of the zeta potential occurred (see Figure 3C, see Table S3). The agglomerate sizes were comparable to reference values.[52,53] Smaller agglomerates caused by PEG are supported by references attributing this effect to steric stabilization.[54–56] Smaller agglomerates lead to a higher accessible surface area, which could lead to higher protein binding capacities. Nevertheless, the surface-related loading increased, too (see Table S3). Hence, it seems that the higher loading could not be attributed to the changed properties of the MNPs, but mainly to the PEG influence on the proteins. In a reference experiment, it was observed that E_8-VHH precipitated at 10% PEG 6000 and pH 5.5 (see Figure S7).

The precipitation of proteins via PEG is well known and ascribed to a higher excluded volume.[34] Lee et al. found out that the protein precipitation via PEG enhances the adsorption of proteins towards chromatographic material, which is caused by steric exclusion [35]. Gagnon et al. described improved capturing of IgM with starch-coated magnetic particles after adding PEG.[57] According to our findings, the effects described by Lee and Gagnon et al. are also true for bare magnetic nanoparticles and are explaining the higher loads at PEG presence. In addition, proteins tend to precipitate at a pH near their isoelectric points.[58,59] As most *E. coli* cell proteins have a pI between 4 and 7, proteins will more likely precipitate at pH 5.5.[60] Adsorption is even more enhanced at the isoelectric points of the proteins.[35] As a consequence, this effect leads to the observed higher loads at pH 5.5 in our studies. This is in good agreement with another reference, which used the latter effect to obtain higher loads on magnetic nanoparticles.[61] Further reference experiments on silica- and oleate-coated MNPs were performed to validate the influence of the MNP surface on binding PEG precipitated proteins. We could observe almost no protein binding to the silica-coated MNPs (3 mg g^{-1}), but a similar binding to the oleate-coated MNPs (130 mg g^{-1}) (see Table S4).

PEG and magnetic nanoparticles are also used in magnetic ATPS. Our manuscript focused on the precipitation of proteins by PEG and not the partitioning of the proteins in the PEG-rich phase. Precipitation of proteins occurs mainly in ATPS at higher protein concentrations, which results in an additional phase (solid precipitates).[62] In this regard, we would be operating in an ATPS-like system at increased protein precipitation conditions binding the precipitates to the magnetic nanoparticles.

VHH was bound to functionalized magnetic particles by other groups before.[51,63] Khalegi et al. showed a load of approximately 27 mg g^{-1}.[64] A polyglutamate-tagged GFP (E_6-GFP) could be bound from lysate with a load of 60 mg g^{-1} in a similar experimental setup.[27] In this regard, it is necessary to mention that the E_6-GFP has a significantly higher relative concentration in the lysate than the VHH.[27]

The binding of the proteins was further verified by infrared spectroscopy. MNPs incubated with EM showed distinct IR peaks at 1550 and 1628 cm^{-1}, indicating the presence of proteins in both samples with and without PEG (see dark blue and dark orange line at Figure 4A and B). Those two specific peaks have often been ascribed to the amide II band and amide I, respectively.[65] It is further assumed that medium components bind to MNPs, indicated by distinct peaks at 1508 and 1601 cm^{-1} for the reference samples (light blue and light orange line at Figure 4A and B). Additionally, the adsorption of PEG was assumed because of the sharp peaks at 1108 and 1343 cm^{-1}, as they appear in the PEG powder blank as well (see Figure 4B).[66] In the presence of proteins, no characteristic PEG peaks could be observed. The infrared spectrum from 4000–500 cm^{-1} can be found in the SI (see Figure S6).

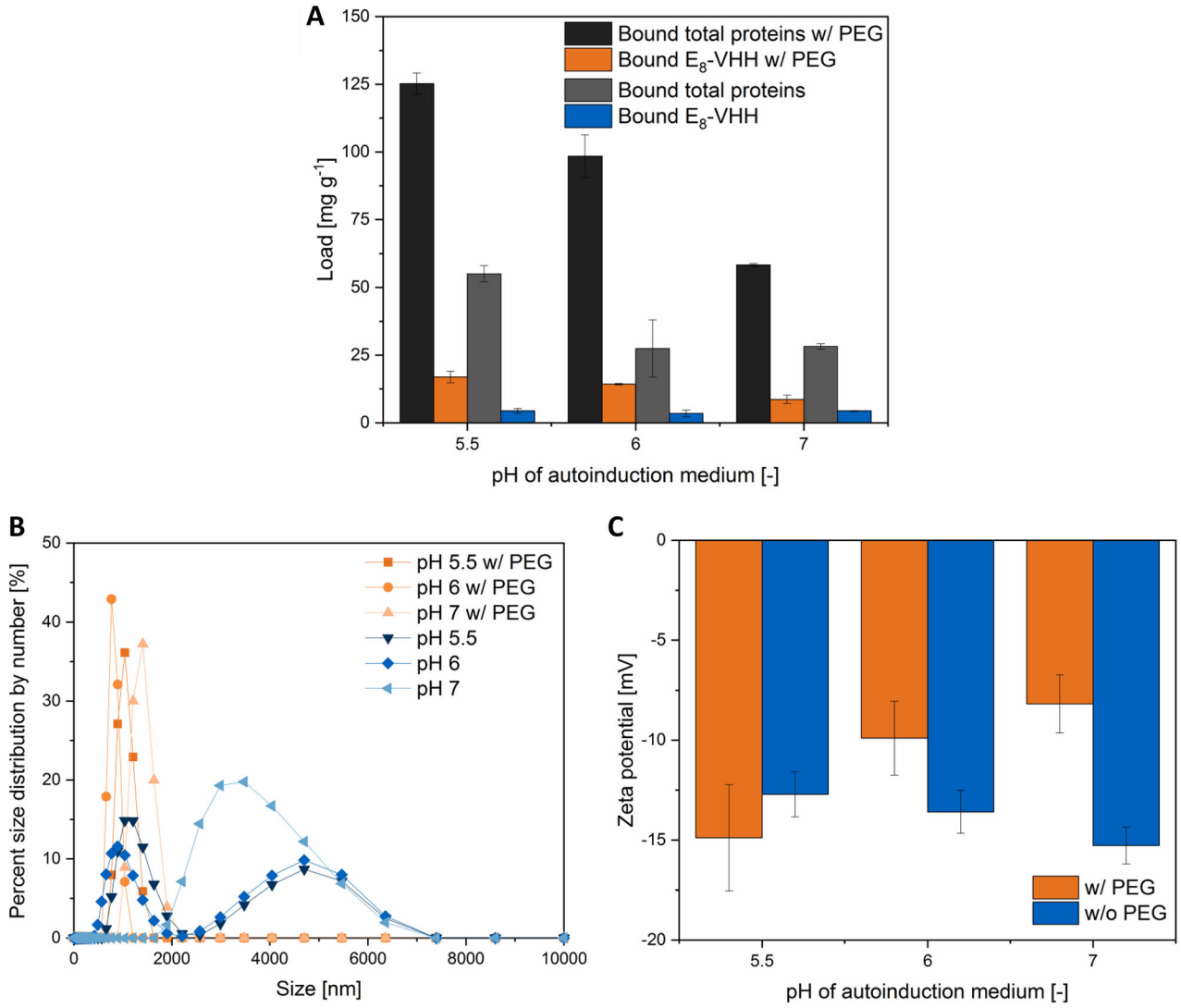

FIGURE 3 Influence of PEG and pH (5.5, 6, 7) on the binding of E_8-VHH and total proteins to the MNPs. (A) Total protein and E_8-VHH load on MNPs. Same experimental conditions as explained in Figure 2. (B) Size distribution (by number) of MNPs measured in autoinduction medium at different pH and with or without PEG 6000 (10% w/v) added. DLS measurement with a ZetaSizer. (C) Zeta potentials of MNPs in conditions described in (B). Standard deviations derive from technical duplicates determined as analytical quintuplicates each

3.3 | Selective elution of the polyglutamate-tagged nanobody

The polyglutamate-tag showed a distinct selective behavior when increasing the concentration ratio of EM to magnetic nanoparticles without PEG. By increasing this ratio, the load on the MNPs and the purity of E_8-VHH could be increased (see Figure 5A and Figure S8). Conversely, the yield was highest at the lowest rate (0.16) (see Figure S8). The higher purity of E_8-VHH at overloading conditions indicates the high selectivity of the E_8-tag, enabling the VHH to outcompete other proteins. In protein corona discussions, the replacement of proteins with lower affinity by proteins with a higher affinity at higher ratios is well known.[67,68] This becomes particularly clear when looking at Figure 5B. At a ratio of 1.8, the E_8-VHH purity jumped from 7.7% to 50% resulting in a purification factor of 6.5 (see Figure 5B, lane 2), whereas a ratio of 0.31 revealed a lower purification factor (see Figure 5B, lane 1).

For an improved purification protocol, we adsorbed E_8-VHH with supplemented PEG (see Figure 5C, lane B) and eluted the E_8-VHH selectively with phosphate buffer (see Figure 5C, lane E). With this approach, the E_8-VHH could be eluted (at 100 mM PBS pH 8.0), whereas 82% of the total proteins remained bound (Figure 5C, lane BE). In contrast, the E_8-VHH did not refold/elute selectively after being precipitated without MNPs (w/ 10% PEG 6000, pH 5.5) or bound to oleate-coated MNPs (see Figure S7 and S9). Additionally, the polyanionic tags are known to increase the solubility of its fusion protein, and thus, the E_8-tag could also help desorbing/ resolubilizing the VHH from the bare MNP surface.[69,70] Without any optimization, we could bind 60% of E_8-VHH and elute 44% of the bound VHH, while having a concentration factor of 5.1 and a purification factor of 4.0 (see Table S5). We hypoth-

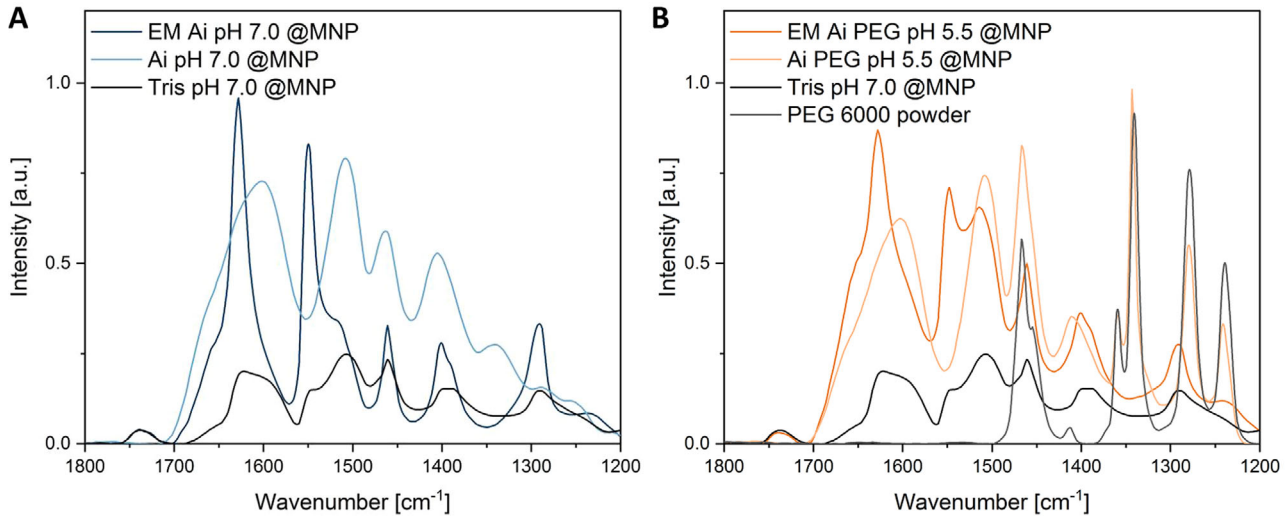

FIGURE 4 Infrared spectra of MNPs incubated with extracellular medium and blanks. Infrared spectra of MNPs contacted with different surroundings (autoinduction medium pH 7, (A) and autoinduction medium with 10% PEG and pH 5.5, (B), washed two times and resuspended in Tris (pH 7.0, 50 mM). Bound EM = Extracellular medium of E_8-VHH expressed in X-press V2, Ai = autoinduction medium blank, PEG = 10% (w/v) PEG 6000 added. The IR spectra were related to the MNP peak at around 590 cm^{-1} except for the PEG powder which was related to the peak at 1341 cm^{-1}

esize that the E_8-VHH binds specifically because of the polyglutamate-tag via monodentate and bidentate bridging coordination.[25] In contrast, the other proteins bind mainly by hydrophobic interactions to the magnetic nanoparticles (see Figure 5D). By being bound via the polyglutamate tag, the tag's characteristic elution behavior with phosphate buffer can be used[27] to elute the E_8-VHH selectively (see Figure 5C, lane E, Figure 5D). The phosphate ions form strong complexes with iron oxides.[71] These bonds are caused by di- and trivalent anions and are stronger than the binding of the polyglutamate tag, which is mainly caused via monodentates.[25,27,71] As a consequence, the phosphate elutes the E_8-VHH by displacement. The other proteins remain bound as their attraction to the magnetic nanoparticles is higher than to the hydrophilic solvent. This hypothesis was further supported by the elution behavior of bound proteins on oleate-coated magnetic nanoparticles, where E_8-VHH did not elute selectively. In detail, the purity of E_8-VHH in the elution fraction of oleate-coated MNPs is 3.3 times lower compared with non-functionalized MNPs (see Figure S9). Selective elution has been previously reported to be a highly efficient purification technique.[72,73] The commonly used His-tag purification strategy yields higher purities than the ones observed in this study.[74] However, a few considerations need to be taken into account. Firstly, the E_8-VHH had a very low initial purity in the lysate, and our approach could enhance the purity significantly (up to 6.5-fold). Secondly, the purification via IMAC requires functionalized matrices (in most cases Ni-NTA functionalization), which are costly.[74] In contrast, no functionalization is needed with our approach as it only requires low-cost magnetic iron oxide nanoparticles originating from a cheap and straightforward co-precipitation synthesis. Additionally, the elution of the polyglutamate-tagged protein can be performed by simply switching the buffer to phosphate, whereas the common elution in IMAC is performed with the hazardous substance imidazole.

4 | CONCLUSION

We are the first to demonstrate the efficient capture of a polyglutamate-tagged nanobody with low-cost, non-functionalized magnetic nanoparticles after being secreted by the enGenes-X-press strain. Like Kastenhofer et al. it was observed that the enGenes-X-press system is a highly potent expression strain that can replace conventional *E. coli* strains since it enabled secretion of the nanobody.[14] We could significantly increase the yield of bound VHH through affinity magnetic precipitation. For this, we added 10% PEG 6000 and decreased the pH of the medium. It was observed that PEG hardly changed the behavior of the magnetic nanoparticles, whereas the proteins precipitated in the presence of PEG. The combination of pH adjustment and PEG addition led to an almost irreversible binding of the host cell proteins, whereby the E_8-VHH could be eluted selectively with phosphate buffer. Selective elution or selective refolding was not possible when bound to oleate-coated magnetic nanoparticles or precipitated without MNPs. The selectivity of the polyglutamate-tag was further seen at overloading conditions, which increased the purification factor up to 6.5. We could bind 60% of E_8-VHH while raising the concentration factor (5x) and purification factor (4x) after eluting the E_8-VHH. Our proof of principle emphasizes using the polyglutamate-tag as fusion tag for extracellularly produced proteins and the subsequent capturing by non-functionalized MNPs. Our findings conclude the promising combination of the enGenes-X-press strains, the polyglutamate-tag, and bare MNPs for proteins in general, not just nanobodies. Moreover, the in situ product removal (ISPR) of secreted proteins with magnetic nanoparticles, as shown by Gädke et al. would be highly interesting with our system.[75] Undoubtedly, further process optimization, such as the variation of precipitation or more elaborate selective elution could result in higher purities and

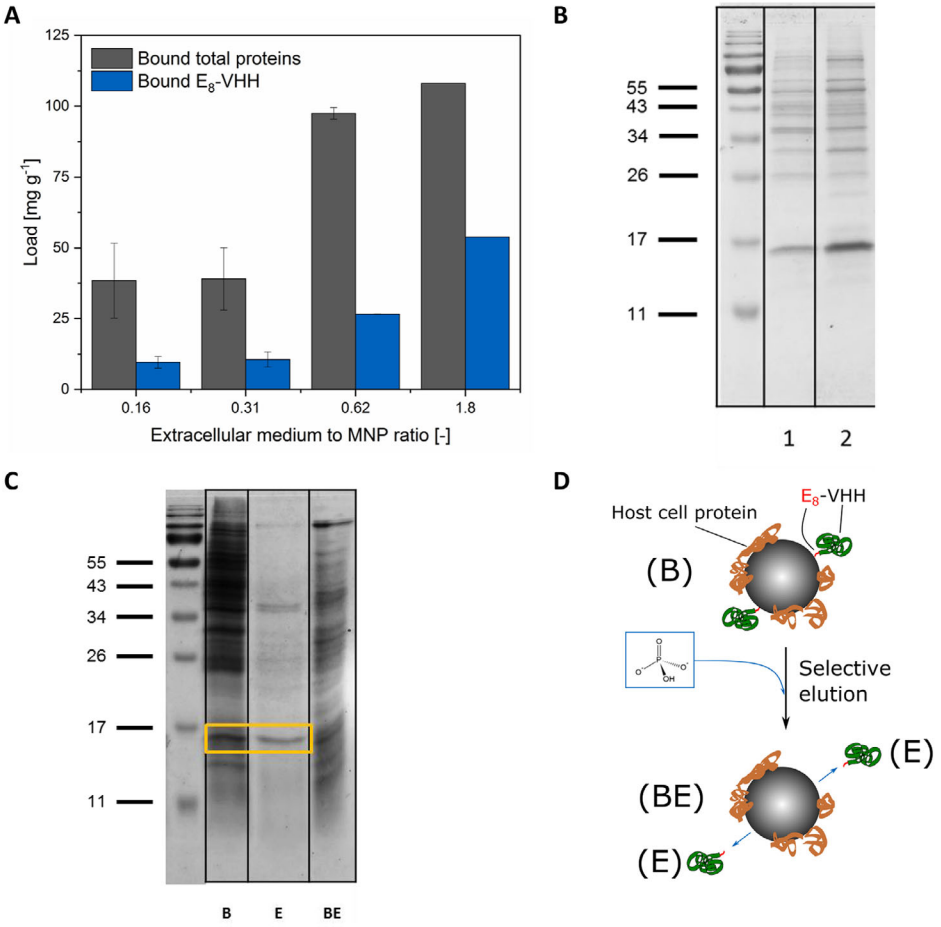

FIGURE 5 The affinity of the polyglutamate-tag and the selective elution. (A) Influence of varied ratios of extracellular medium (EM) to MNP for incubation. Load of the total proteins and E_8-VHH on the MNPs after incubation (1 h, 25°C, 1000 rpm) and two times washing with 50 mM Tris pH 7.0. The total protein load was obtained from technical duplicates measured as analytical triplicates via particle-BCA each. The point 1.8 was received from one replicate. The E_8-VHH load was calculated from the total protein load multiplied with the densitometric purity of the E_8-VHH spot with SDS-PAGE obtained from both technical duplicates. (B) SDS-PAGE of E_8-VHH cultivated in X-press V2 (autoinduction medium) and its extracellular medium contacted with 1 g L^{-1} MNPs for 1 h (25°C, 1000 rpm). The EM:MNP ratio was 0.31 (lane 1) and 1.8 (lane 2). The overloading of MNPs results in a higher VHH purity. (C) SDS-PAGE of E_8-VHH cultivated in X-press V2 and PEG 6000 (10% w/v) was added to its extracellular medium, adjusted to pH 5.5 and afterwards contacted with 1 g/L MNPs for 1 h (25°C, 1000 rpm). The experiment was performed in a 1.8 mL scale. The MNP-bound proteins after contacting and two times washing (B) and the eluted proteins € from the (B)-samples and still bound proteins after elution (BE) were loaded onto a 15% gel. (D) Scheme of the selective elution where E_8-VHH is specifically bound to the magnetic nanoparticles via the polyglutamate-tag, whereas the other proteins are bound non-specifically (B = bound). The specific binding allows for an elution with phosphate buffer (E = eluted) for the E_8-VHH while the other proteins remain bound (BE = still bound after elution)

yields, which is of future interest and would enhance the utility of the method. It would be exciting to try out a more continuous approach by retaining the cells and contacting the EM with MNPs. Moreover, the presence of PEG and magnetic nanoparticles allows the combination of magnetic ATPS or magnetic micellar ATPS, which was not further studied in this manuscript, but holds great potential, too. It may also be worth evaluating our process for other proteins having different properties.

ACKNOWLEDGMENTS

The authors would like to thank Lucia Abarca-Cabrera for providing the oleate-coated magnetic iron oxide nanoparticles. The synthesis and characterization of silica-coated magnetic nanoparticles was experimentally supported by Michaela Mitzkus, Carsten Peters, Matthias Opel, and financially supported by TUM International Graduate School of Science and Engineering (IGSSE). We thank Maximilian Zwiebel and Matthias Mann from the Max-Planck Institute of Biochemistry to identify the E_8-VHH via mass spectrometry and Paula Fraga-Garcia for her valuable ideas concerning the discussion. We are also grateful for the laboratory work of Tuan Hoang Son regarding the E_8-VHH expression experiments and the language editing by Tobias Steegmüller. Moreover, we are especially grateful for the financial support of the Federal Ministry of Education and Research (Grant number 031B0521A) and for the support from the Marie Skłodowska Curie actions of the European Commission (project 887412, NERS), which made this research possible.

CONFLICT OF INTEREST

Sonja Berensmeier and Sebastian P. Schwaminger filed a patent application on negatively charged peptide tags. Juergen Mairhofer has filed a patent on the reported enGenes-X-press technology [PCT/EP2016/059597] and owns interests in enGenes Biotech. enGenes Biotech is the legal entity commercializing the reported X-press technology.

DATA AVAILABILITY STATEMENT

The data that support the findings of this study are available from the corresponding author upon reasonable request.

ORCID

Alexander A. Zanker https://orcid.org/0000-0002-7855-2978
Sebastian P. Schwaminger https://orcid.org/0000-0002-8627-0807
Sonja Berensmeier https://orcid.org/0000-0002-4943-848X

REFERENCES

1. Li, H., Er Saw, P., & Song, E. (2020). Challenges and strategies for next-generation bispecific antibody-based antitumor therapeutics. *Cellular and Molecular Immunology*, *17*(5), 451–461.
2. Bracken, C. J., Lim, S. A., Solomon, P., Rettko, N. J., Nguyen, D. P., Zha, B. S., Schaefer, K., Byrnes, J. R., Zhou, J., Lui, I., Liu, J., Pance, K., Azumaya, C. M., Braxton, J. R., Brilot, A. F., Gupta, M., Li, F., Lopez, K. E., Melo, A.,… , Q.S.B. Consortium, E.M.G.F.C.T. Cryo, E.M.D.P.T. Cryo, T. Mammalian Cell Expression, T. Protein Purification, T. Crystallography, T. Bacterial Expression, T. Infrastructure, T. Leadership (2021). Bi-paratopic and multivalent vh domains block ace2 binding and neutralize sars-cov-2. *Nature Chemical Biology*, *17*(1), 113–121.
3. Holliger, P., & Hudson, P. J. (2005). Engineered antibody fragments and the rise of single domains. *Nature Biotechnology*, *23*(9), 1126–1136.
4. Muyldermans, S. (2013). Nanobodies: Natural single-domain antibodies. *Annual Review of Biochemistry*, *82*(1), 775–797.
5. Shriver-Lake, L. C., Goldman, E. R., Zabetakis, D., & Anderson, G. P. (2017). Improved production of single domain antibodies with two disulfide bonds by co-expression of chaperone proteins in the escherichia coli periplasm. *Journal of Immunological Methods*, *443*, 64–67.
6. De Genst, E., Silence, K., Decanniere, K., Conrath, K., Loris, R., Kinne, J., Muyldermans, S., & Wyns, L. (2006). Molecular basis for the preferential cleft recognition by dromedary heavy-chain antibodies. *Proceedings of the National Academy of Sciences of the United States*, *103*(12), 4586–4591.
7. Kunz, P., Zinner, K., Mücke, N., Bartoschik, T., Muyldermans, S., & Hoheisel, J. D. (2018). The structural basis of nanobody unfolding reversibility and thermoresistance. *Science Reports*, *8*(1), 7934.
8. Liu, Y., & Huang, H. (2018). Expression of single-domain antibody in different systems. *Applied Microbiology and Biotechnology*, *102*(2), 539–551.
9. Frenzel, A., Hust, M., Schirrmann, T. (2013). Expression of recombinant antibodies. *Frontiers in Immunology*, *4*(217).
10. De Marco, A. (2020). Recombinant expression of nanobodies and nanobody-derived immunoreagents. *Protein Expression and Purification*, *172*, 105645–105645.
11. Tian, B., Wong, W. Y., Uger, M. D., Wisniewski, P., & Chao, H. (2017). Development and characterization of a camelid single domain antibody–urease conjugate that targets vascular endothelial growth factor receptor 2. *Frontiers in Immunology*, *8*(956).
12. Ruano-Gallego, D., Fraile, S., Gutierrez, C. et al. (2019). Screening and purification of nanobodies from E. coli culture supernatants using the hemolysin secretion system. *Microb Cell Fact*, *18*, 47. https://doi.org/10.1186/s12934-019-1094-0.
13. Kleiner-Grote, G. R. M., Risse, J. M., & Friehs, K. (2018). Secretion of recombinant proteins from E. Coli. *Engineering in Life Sciences*, *18*(8), 532–550.
14. Kastenhofer, J., Rettenbacher, L., Feuchtenhofer, L., Mairhofer, J., & Spadiut, O. (2021). Inhibition of E. Coli host rna polymerase allows efficient extracellular recombinant protein production by enhancing outer membrane leakiness. *Biotechnology Journal*, *16*(3), 2000274.
15. Stargardt, P., Feuchtenhofer, L., Cserjan-Puschmann, M., Striedner, G., & Mairhofer, J. (2020). Bacteriophage inspired growth-decoupled recombinant protein production in escherichia coli. *ACS Synthetic Biology*, *9*(6), 1336–1348.
16. Salema, V., & Fernández, L. (2013). High yield purification of nanobodies from the periplasm of E. Coli as fusions with the maltose binding protein. *Protein Expression and Purification*, *91*(1), 42–48.
17. Safarik, I., & Safarikova, M. (2004). Magnetic techniques for the isolation and purification of proteins and peptides. *BioMagnetic Research and Technology*, *2*(1), 7.
18. Saraswat, M., Musante, L., Ravidá, A., Shortt, B., Byrne, B., & Holthofer, H. (2013). Preparative purification of recombinant proteins: Current status and future trends. *BioMed Research International*, *2013*, 312709–312709.
19. Franzreb, M., Siemann-Herzberg, M., Hobley, T. J., & Thomas, O. R. T. (2006). Protein purification using magnetic adsorbent particles. *Applied Microbiology and Biotechnology*, *70*(5), 505–516.
20. Kaveh-Baghbaderani, Y., Allgayer, R., Schwaminger, S. P., Fraga-García, P., & Berensmeier, S. (2021). Magnetic separation of antibodies with high binding capacity by site-directed immobilization of protein a-domains to bare iron oxide nanoparticles. *ACS Applied Nano Materials*, *4*(5), 4956–4963.
21. Schwaminger, S. P., Fraga-García, P., Eigenfeld, M., Becker, T. M., & Berensmeier, S. (2019). Magnetic separation in bioprocessing beyond the analytical scale: From biotechnology to the food industry. *Frontiers in Bioengineering*, *7*(233).
22. Bohara, R. A., Thorat, N. D., & Pawar, S. H. (2016). Role of functionalization: Strategies to explore potential nano-bio applications of magnetic nanoparticles. *RSC Advances*, *6*(50), 43989–44012.
23. Schwaminger, S. P., Fraga-García, P., Blank-Shim, S. A., Straub, T., Haslbeck, M., Muraca, F., Dawson, K. A., & Berensmeier, S. (2019). Magnetic one-step purification of his-tagged protein by bare iron oxide nanoparticles. *ACS Omega*, *4*(2), 3790–3799.
24. Blank-Shim, S. A., Schwaminger, S. P., Borkowska-Panek, M., Anand, P., Yamin, P., Fraga-García, P., Fink, K., Wenzel, W., & Berensmeier, S. (2017). Binding patterns of homo-peptides on bare magnetic nanoparticles: Insights into environmental dependence. *Science Reports 7*(1), 14047.
25. Schwaminger, S. P., Blank-Shim, S. A., Scheifele, I., Fraga-García, P., & Berensmeier, S. (2017). Peptide binding to metal oxide nanoparticles. *Faraday Discussions 204*(0), 233–250.
26. Schwaminger, S. P., García, P. F., Merck, G. K., Bodensteiner, F. A., Heissler, S., Günther, S., & Berensmeier, S. (2015). Nature of interactions of amino acids with bare magnetite nanoparticles. *Journal of Physical Chemistry*, *119*(40), 23032–23041.
27. Schwaminger, S. P., Blank-Shim, S. A., Scheifele, I., Pipich, V., Fraga-García, P., & Berensmeier, S. (2019). Design of interactions between nanomaterials and proteins: A highly affine peptide tag to bare iron oxide nanoparticles for magnetic protein separation. *Biotechnology Journal*, *14*(3), 1800055.
28. Santos, R. D., Iria, I., Manuel, A. M., Leandro, A. P., Madeira, C.a.C., Goncalves, J., Carvalho, A. L., & Roque, A. C. A. (2020). Magnetic precipitation: A new platform for protein purification. *Biotechnology Journal*, *15*(9), 2000151.

29. Flygare, S., Wikström, P., Johansson, G., & Larsson, P. O. (1990). Magnetic aqueous two-phase separation in preparative applications. *Enzyme and Microbial Technology*, *12*(2), 95–103.
30. Wikström, P., Flygare, S., Gröndalen, A., & Larsson, P.-O. (1987). Magnetic aqueous two-phase separation: A new technique to increase rate of phase-separation, using dextran-ferrofluid or larger iron oxide particles. *Analytical Biochemistry*, *167*(2), 331–339.
31. Dhadge, V. L., Rosa, S. A. S. L., Azevedo, A., Aires-Barros, R., & Roque, A. C. A. (2014). Magnetic aqueous two phase fishing: A hybrid process technology for antibody purification. *Journal of Chromatography A*, *1339*, 59–64.
32. Becker, J. S., Thomas, O. R. T., & Franzreb, M. (2009). Protein separation with magnetic adsorbents in micellar aqueous two-phase systems. *Separation and Purification Technology*, *65*(1), 46–53.
33. Suzuki, M., Kamihira, M., Shiraishi, T., Takeuchi, H., & Kobayashi, T. (1995). Affinity partitioning of protein a using a magnetic aqueous two-phase system. *Journal of Fermentation and Bioengineering*, *80*(1), 78–84.
34. Kumar, V., Sharma, V. K., & Kalonia, D. S. (2009). Effect of polyols on polyethylene glycol (peg)-induced precipitation of proteins: Impact on solubility, stability and conformation. *International Journal of Pharmaceutics*, *366*(1), 38–43.
35. Lee, J., Gan, H. T., Latiff, S. M., Chuah, C., Lee, W. Y., Yang, Y. S., Loo, B., Ng, S. K., & Gagnon, P. (2012). Principles and applications of steric exclusion chromatography. *Journal of Chromatography A*, *1270*, 162–170.
36. Atha, D. H., & Ingham, K. C. (1981). Mechanism of precipitation of proteins by polyethylene glycols. Analysis in terms of excluded volume. *Journal of Biological Chemistry*, *256*(23), 12108–12117.
37. Stargardt, P., Striedner, G., & Mairhofer, J. (2021). Tunable expression rate control of a growth-decoupled t7 expression system by l-arabinose only. *Microbial Cell Factories*, *20*(1), 27.
38. Thomas, J. A., Schnell, F., Kaveh-Baghbaderani, Y., Berensmeier, S., & Schwaminger, S. P. (2020). Immunomagnetic separation of microorganisms with iron oxide nanoparticles. *Chemosensors*, *8*(1).
39. Schwaminger, S. P., Schwarzenberger, K., Gatzemeier, J., Lei, Z., & Eckert, K. (2021). Magnetically induced aggregation of iron oxide nanoparticles for carrier flotation strategies. *ACS Applied Materials & Interfaces*, *13*(17), 20830–20844.
40. Chung, C. T., Niemela, S. L., & Miller, R. H. (1989). One-step preparation of competent Escherichia coli: Transformation and storage of bacterial cells in the same solution. *PNAS*, *86*(7), 2172.
41. Toeroek, C., Cserjan-Puschmann, M., Bayer, K., & Striedner, G. (2015). Fed-batch like cultivation in a micro-bioreactor: Screening conditions relevant for escherichia coli based production processes. *SpringerPlus*, *4*(1), 490.
42. Ames, G. F., Prody, C., & Kustu, S. (1984). Simple, rapid, and quantitative release of periplasmic proteins by chloroform. *Journal of Bacteriology*, *160*(3), 1181–1183.
43. Bradford, M. M. (1976). A rapid and sensitive method for the quantitation of microgram quantities of protein utilizing the principle of protein-dye binding. *Analytical Biochemistry*, *72*(1), 248–254.
44. Shevchenko, A., Tomas, H., Havli, J., Olsen, J. V., & Mann, M. (2006). In-gel digestion for mass spectrometric characterization of proteins and proteomes. *Nature Protocols*, *1*(6), 2856–2860.
45. Wiśniewski, J. R., & Mann, M. (2012). Consecutive proteolytic digestion in an enzyme reactor increases depth of proteomic and phosphoproteomic analysis. *Analytical Chemistry*, *84*(6), 2631–2637.
46. Regupathi, I., Govindarajan, R., Pandian Amaresh, S., & Murugesan, T. (2009). Densities and viscosities of polyethylene glycol 6000 + triammonium citrate + water systems. *Journal of Chemical and Engineering Data*, *54*(12), 3291–3295.
47. Baek, M., Dimaio, F., Anishchenko, I., Dauparas, J., Ovchinnikov, S., Lee, G. R., Wang, J., Cong, Q., Kinch, L. N., Schaeffer, R. D., Millán, C., Park, H., Adams, C., Glassman, C. R., Degiovanni, A., Pereira, J. H., Rodrigues, A. V., Dijk, A.a.V., Ebrecht, A. C., … Baker, D. (2021). Accurate prediction of protein structures and interactions using a three-track neural network. *Science*, *373*(6557), 871–876.
48. Maggi, M., & Scotti, C. (2017). Enhanced expression and purification of camelid single domain vhh antibodies from classical inclusion bodies. *Protein Expression and Purification*, *136*, 39–44.
49. Noguchi, T., Nishida, Y., Takizawa, K., Cui, Y., Tsutsumi, K., Hamada, T., & Nishi, Y. (2017). Accurate quantitation for in vitro refolding of single domain antibody fragments expressed as inclusion bodies by referring the concomitant expression of a soluble form in the periplasms of escherichia coli. *Journal of Immunological Methods*, *442*, 1–11.
50. Anderson, G. P., Liu, J. L., Shriver-Lake, L. C., Zabetakis, D., Sugiharto, V. A., Chen, H.-W., Lee, C.-R., Defang, G. N., Wu, S.-J. L., Venkateswaran, N., & Goldman, E. R. (2019). Oriented immobilization of single-domain antibodies using spytag/spycatcher yields improved limits of detection. *Analytical Chemistry*, *91*(15), 9424–9429.
51. Zhu, M., Hu, Y., Li, G., Ou, W., Mao, P., Xin, S., & Wan, Y. (2014). Combining magnetic nanoparticle with biotinylated nanobodies for rapid and sensitive detection of influenza h3n2. *Nanoscale Research Letters*, *9*(1), 528.
52. Mbeh, D. A., Javanbakht, T., Tabet, L., Merhi, Y., Maghni, K., Sacher, E., & Yahia, L. H. (2015). Protein corona formation on magnetite nanoparticles: Effects of culture medium composition, and its consequences on superparamagnetic nanoparticle cytotoxicity. *Journal of Biomedical Nanotechnology*, *11*(5), 828–840.
53. Zanker, A. A., Ahmad, N., Son, T. H., Schwaminger, S. P., & Berensmeier, S. (2021). Selective ene-reductase immobilization to magnetic nanoparticles through a novel affinity tag. *Biotechnology Journal*, *16*(4), 2000366.
54. García-Jimeno, S., & Estelrich, J. (2013). Ferrofluid based on polyethylene glycol-coated iron oxide nanoparticles: Characterization and properties. *Colloids and Surfaces*, *420*, 74–81.
55. Cornell, R. M., & Schwertmann, U. (2003). Surface chemistry and colloidal stability, in *The iron oxides*. (pp. 221–252).
56. Kharisov, B. I., Dias, H. V. R., Kharissova, O. V., Vázquez, A., Peña, Y., & Gómez, I. (2014). Solubilization, dispersion and stabilization of magnetic nanoparticles in water and non-aqueous solvents: Recent trends. *RSC Advances*, *4*(85), 45354–45381.
57. Gagnon, P., Toh, P., & Lee, J. (2014). High productivity purification of immunoglobulin g monoclonal antibodies on starch-coated magnetic nanoparticles by steric exclusion of polyethylene glycol. *Journal of Chromatography A*, *1324*, 171–180.
58. Lovrien, R. E., & Matulis, D. (1997). Selective precipitation of proteins. *Current Protocols in Protein Science*, *7*(1), 4.5.1–4.5.36.
59. Cohn, E. J. (1922). Studies in the physical chemistry of the proteins: I. The solubility of certain proteins at their isoelectric points. *Journal of General Physiology*, *4*(6), 697–722.
60. Link, A. J., Robison, K., & Church, G. M. (1997). Comparing the predicted and observed properties of proteins encoded in the genome of escherichia coli k-12. *Electrophoresis*, *18*(8), 1259–1313.
61. Roth, H. C., Schwaminger, S. P., Peng, F., & Berensmeier, S. (2016). Immobilization of cellulase on magnetic nanocarriers. *ChemistryOpen*, *5*(3), 183–187.
62. Asenjo, J. A., & Andrews, B. A. (2011). Aqueous two-phase systems for protein separation: A perspective. *Journal of Chromatography A*, *1218*(49), 8826–8835.
63. Thys, B., Saerens, D., Schotte, L., De Bleeser, G., Muyldermans, S., Hassanzadeh-Ghassabeh, G., & Rombaut, B. (2011). A simple quantitative affinity capturing assay of poliovirus antigens and subviral particles by single-domain antibodies using magnetic beads. *Journal of Virological Methods*, *173*(2), 300–305.
64. Khaleghi, S., Rahbarizadeh, F., Ahmadvand, D., & Hosseini, H. R. M. (2017). Anti-her2 vhh targeted magnetoliposome for intelligent magnetic resonance imaging of breast cancer cells. *Cellular and Molecular Bioengineering*, *10*(3), 263–272.

65. Barth, A. (2007). Infrared spectroscopy of proteins. *Biochim Biophys*, *1767*(9), 1073–1101.
66. Masoudi, A., Madaah Hosseini, H. R., Shokrgozar, M. A., Ahmadi, R., & Oghabian, M. A. (2012). The effect of poly(ethylene glycol) coating on colloidal stability of superparamagnetic iron oxide nanoparticles as potential mri contrast agent. *International Journal of Pharmaceutics*, *433*(1), 129–141.
67. Mahmoudi, M., Lynch, I., Ejtehadi, M. R., Monopoli, M. P., Bombelli, F. B., & Laurent, S. (2011). Protein—nanoparticle interactions: Opportunities and challenges. *Chemical Reviews*, *111*(9), 5610–5637.
68. Lynch, I., & Dawson, K. A. (2008). Protein-nanoparticle interactions. *Nano Today*, *3*(1), 40–47.
69. Paraskevopoulou, V., & Falcone, F. H. (2018). Polyionic tags as enhancers of protein solubility in recombinant protein expression. *Microorganisms*, *6*(2), 47.
70. Han, X., Ning, W., Ma, X., Wang, X., & Zhou, K. (2020). Improving protein solubility and activity by introducing small peptide tags designed with machine learning models. *Metabolic Engineering Communications*, *11*, e00138.
71. Daou, T. J., Begin-Colin, S., Grenèche, J. M., Thomas, F., Derory, A., Bernhardt, P., Legaré, P., & Pourroy, G. (2007). Phosphate adsorption properties of magnetite-based nanoparticles. *Chemistry of Materials*, *19*(18), 4494–4505.
72. Dierickx, P. J. (1990). Selective elution of soluble rat liver glutathione transferases from a glutathione-sepharose affinity column. *Journal of Chromatography B*, *530*, 263–271.
73. Kaleas, K. A., Schmelzer, C. H., & Pizarro, S. A. (2010). Industrial case study: Evaluation of a mixed-mode resin for selective capture of a human growth factor recombinantly expressed in E. Coli. *Journal of Chromatography A*, *1217*(2), 235–242.
74. Bornhorst, J. A., & Falke, J. J. (2000). Purification of proteins using polyhistidine affinity tags. *Methods in Enzymology*, *326*, 245–254.
75. Gädke, J., Kleinfeldt, L., Schubert, C., Rohde, M., Biedendieck, R., Garnweitner, G., & Krull, R. (2017). In situ affinity purification of his-tagged protein a from bacillus megaterium cultivation using recyclable superparamagnetic iron oxide nanoparticles. *Journal of Biotechnology*, *242*, 55–63.

SUPPORTING INFORMATION

Additional supporting information may be found in the online version of the article at the publisher's website.

How to cite this article: Zanker, A. A., Stargardt, P., Kurzbach, S. C., Turrina, C., Mairhofer, J., Schwaminger, S. P., & Berensmeier, S. (2022). Direct capture and selective elution of a secreted polyglutamate-tagged nanobody using bare magnetic nanoparticles. *Biotechnology Journal*, *17*, e2100577. https://doi.org/10.1002/biot.202100577